analytical chemistry

Article

Cite This: Anal. Chem. XXXX, XXX, XXX−XXX

pubs.acs.org/ac

Detection and Identification of Fungal Infections in Intact Wheat and Sorghum Grain Using a Hand-Held Raman Spectrometer

Veronica Egging,[†] Jasmine Nguyen,[†] and Dmitry Kurouski*[,†,‡]

[†]Department of Biochemistry and Biophysics, Texas A&M University, College Station, Texas 77843, United States

[‡]The Institute for Quantum Science and Engineering, Texas A&M University, College Station, Texas 77843, United States

Supporting Information

ABSTRACT: Global population growth drives increasing food demand, which is anticipated to increase by at least 20% over the next 15 years. Rapid detection and identification of plant pathogens allows for up to a 50% increase in the total agricultural yield worldwide. Current molecular methods for pathogen diagnostics, such as polymerase chain reaction (PCR), are costly, time-consuming, and destructive. These limitations recently catalyzed a push toward developing minimally invasive and substrate general techniques that can be used in the field for confirmatory detection and identification of plant pathogens. Raman spectroscopy (RS) is a noninvasive, nondestructive, and label-free technique that can be used to determine chemical structure of analyzed specimens. In this study, we demonstrate that by using a hand-held Raman spectrometer, we can identify whether wheat or sorghum grains are healthy or not and identify present plant pathogens. We show that RS enables diagnosis of simple diseases, such as ergot, that are caused by one pathogen, as well as complex diseases, such as black tip or mold, which are induced by several different pathogens. The combination of chemometric analysis and RS allows for distinguishing between healthy and infected grains with high accuracy. We also show that RS can be used to determine states of disease development on grain. These results demonstrate that Raman-based approach for disease detection on plants is sample agnostic.

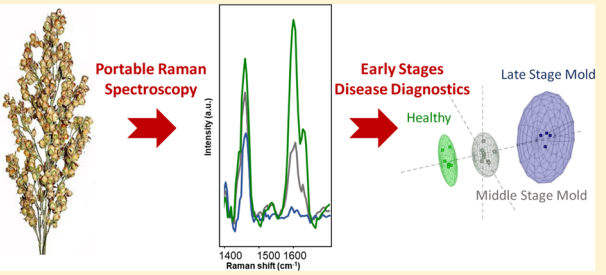

Global population growth places increasing pressure on food production. Relieving this pressure can be achieved by methods such as via deforestation and expansion of agricultural lands or timely treatment of crop diseases, which cause 20−40% loss of total agricultural yield worldwide.[1] Current technologies for identification of plant pathogens include indirect and direct methods.[2] Indirect approaches detect plant responses to pathogens, such as change of color or temperature, and include thermography,[3] hyperspectral imagery,[4] and visible, infrared or fluorescence spectroscopy.[2] By attaching the relevant instrumentation to an unmanned aerial vehicle (UAV), large tracts of land can be quickly surveyed. However, these methods cannot identify specific pathogens.

Direct methods for detection and identification of plant pathogens include flow cytometry, gas and liquid chromatography coupled with mass-spectrometry (GC- and LC-MS),[5] enzyme-linked immunosorbent assay (ELISA),[6] immunofluorescence,[7] fluorescence in situ hybridization (FISH),[8] and polymerase chain reaction (PCR).[9,10] These exhibit high pathogen specificity; however, they have their own limitations. Specifically, PCR is highly sensitive to contamination from environmental DNA, can be inhibited by small quantities of organic solvents and requires initial design of primers based on known DNA sequences. It has limited portability and is essentially destructive to the analyzed specimens.[2,9] The chemical dyes used in immunofluorescence, FISH and ELISA are highly sensitive to photobleaching. Additionally, these techniques typically cannot detect all pathogens.[2] Flow cytometry requires analyzed material be in suspension and often generates excessive amount of data, making sample analysis complicated.[7,11] GC- and LC-MS are costly, destructive, and have limited portability.[5,12] Lack of noninvasive, nondestructive, confirmatory technology to detect plant infection is what sparked and challenged us to investigate the capacity of Raman spectroscopy to solve this problem.

Raman spectroscopy (RS) is a modern analytical technique that provides information about molecular vibrations and consequently the structure of the analyzed specimen. The Raman effect is based on inelastic scattering of photons by molecules that are being excited to higher vibrational or rotational states. RS has been broadly used in various research fields ranging from forensic analysis of bodily fluids[13−15] and pesticides[16] to food science[17] and electrochemistry.[18] Recently, several companies[19,20] produced hand-held Raman spectrometers. This enables utilization of RS directly in the field for applications, such as forensics[21,22] and mineralogy.[23,24]

Our group recently demonstrated that, using a hand-held Raman system, we were able to detect and identify plant diseases on maize.[25] Specifically, we were able to identify

Received: April 25, 2018
Accepted: June 13, 2018
Published: June 13, 2018

DOI: 10.1021/acs.analchem.8b01863
Anal. Chem. XXXX, XXX, XXX−XXX

whether maize kernels were healthy of infected by *Aspergillus flavus*, *A. niger*, *Fusarium spp.*, or *Diplodia spp.* with 100% accuracy. We chose to further our studies using a hand-held Raman system on wheat and sorghum seeds because these crops are the most economically important food sources grown worldwide.[26,27]

In this study, we investigated wheat and sorghum grains infected with ergot, black tip, or mold. These pathogens cause devastating losses (up to 50% of crop yield) in both wheat[28] and sorghum.[29] Ergot infection is caused by *Clavicepus sp.*[30] that forms sclerotia on the surface of infected grain. Ergot sclerotia produce highly toxic alkaloids which cause severe muscle spasms, fever, hallucinations, mania, paralysis, tremors, distorted perceptions, and even reduce human fertility and cause spontaneous abortions.[31] Therefore, sclerotia content must be controlled. For instance, in the United States, wheat cannot contain more than 0.05% sclerotia by weight.[32] Black tip disease is associated with *Alternaria spp., Cochliobolus spp.,* and *Cladosporium spp.*[33,34] It is characterized by a blackening of the embryo of wheat kernels and occurs in wet, humid environments. This disease reduces weight of grains, economic worth, and in some cases decreases seed germination.[34] Furthermore, if a grain infected with *Cochliobolus sativus* is planted, it can lead to seedling blights. Losses of sorghum grain to mold infection are estimated to vary from 30% to 100% and cost Asia and Africa 130 million US dollars.[35] As in black tip, economic losses are due to decreased seed mass, density, and germination chance. Grain mold infection is caused by a variety of different fungal species including *Fusarium andiyazi*, *F. proliferatum*, *F. sacchari*, *F. verticillioides*, and *F. thapsinum*,[35] which colonize developing grain in wet or humid conditions.[36] Because of the number of contributing pathogens, accurate and early identification of individual causative agents is not always possible using conventional methods, such as PCR, which targets specific nucleotide sections of each pathogen.

In this study, we examined simple and complex diseases. Simple diseases, such as ergot, are caused by a single pathogen, whereas complex diseases, including black tip and mold, are caused by multiple pathogens. We demonstrated that by using a portable Raman spectrometer we not only could detect and identify simple-case pathogen disease but also diagnosed complex plant diseases such as black tip and mold. Moreover, such examination is label-free, noninvasive, and nondestructive to the analyzed grain.

EXPERIMENTAL SECTION

Materials. Healthy and disease-infected wheat and sorghum grain was provided by laboratories of Prof. Isakeit from the Department of Plant Pathology and Microbiology and Prof. Ibrahim from the Department of Soil and Crop Sciences, Texas A&M University. Plant diseases, as well as stages of their progression on grain, were confirmed and determined by samples' examination performed by the expert in plant pathology Prof. Isakeit based on disease discrete phenotypic appearance.

Spectroscopy. Raman spectra were collected with a hand-held portable Rigaku Progeny ResQ spectrometer (Rigaku Analytical Devices, Inc. Wilmington, MA), equipped with a 1064 nm Nd:YAG laser. The following experimental parameters were used for all collected Raman spectra: 1064 nm excitation wavelength, 80 s acquisition time, 200 mW power, and baseline spectral subtraction by device software. Spectra were taken from the middle of the side of each grain. The number of spectra that comprise each averaged spectra are as follows: Healthy sorghum has 8 spectra averaged, sorghum ergot has 7, sorghum early mold infection has 11, sorghum middle mold infection has 9, sorghum late mold infection has 9, healthy wheat has 7, wheat black tip has 9, and wheat ergot has 8. Spectra were taken from different grains, screened for outliers, and averaged. Spectra shown in the manuscript are raw baseline corrected, without smoothing.

Multivariate Data Analysis. SIMCA 14 (Umetrics, Umeå, Sweden) was used for statistical analysis of the collected Raman spectra. To give all spectral regions equal importance, spectra were scaled to unit variance. Partial least-squares discriminant analysis (PLS-DA) was performed in order to determine the number of significant components and identify spectral regions that best explain the separation between the classes. The analysis was performed in two iterations. In the first iteration, the PLS-DA model was built using all wavenumbers in the recorded spectra. In the second iteration, wavenumbers with a variable importance (VIP) score of less than 1.0 were excluded to reduce noise and improve the predictive power of the model.

Spectral Processing. Processing and averaging were done with GRAMS/AI 7.0 software (Thermo Galactic, Salem, NH).

RESULTS AND DISCUSSION

Detection and Identification of Ergot and Black Tip Infection on Wheat. Raman spectrum of healthy wheat exhibits vibrational bands originating from proteins, pectin, lignin, carbohydrates, and carotenoids (Figure 1A and Table 1).

Raman spectra of ergot- and black tip-infected wheat are very similar to the spectrum of healthy wheat. Nevertheless, we observed significant differences in intensities and frequencies of some vibrational bands associated with proteins, pectin and carotenoids. Raman spectra of proteins typically exhibit several amide vibrations, known as amide I (1640−1670 cm^{-1},), amide II (~1555 cm^{-1}), and amide III (1230−1270 cm^{-1}).[37] The amide I position is sensitive to the secondary structure of the protein molecule. Specifically, an α-helix exhibits the amide I band around 1650 cm^{-1}, whereas the amide I of a β-sheet is typically around 1670 cm^{-1}. In the spectra of ergot-infected wheat, we observed two distinct peaks in the amide I region centered around 1650 and 1667 cm^{-1} that were not evident in the spectra of healthy wheat and black tip (Figure 1B). This observation indicates that ergot infection in the wheat may be associated with expression and deposition of α-helical and β-sheet proteins.

Interestingly, we did not observe significant changes in intensities of vibrational bands associated with lignin and carbohydrates apart from pectin (Table 1) in ergot-infected wheat. This indicates that ergot infection is not associated with significant changes in the structures of these biopolymers upon their growth and development on grains. At the same time, we observed small changes in the vibrational bands of carbohydrates in the spectrum of black tip-infected wheat. Specifically, in the spectra of black tip-infected wheat, the intensity of the vibrational band at 862 and 937 cm^{-1} decreased, whereas the intensities of the vibrational bands at 1348 and 1600 cm^{-1} increased compared to the spectrum of healthy wheat (Figure 1A). Vibrational bands at 862 and 937 cm^{-1} are associated with C−O−C vibration, which is typical for starch, whereas the band at 1348 cm^{-1} corresponds to C−O−H vibration[38] that is characteristic for monomeric sugars. Thus, based on the

DOI: 10.1021/acs.analchem.8b01863
Anal. Chem. XXXX, XXX, XXX−XXX

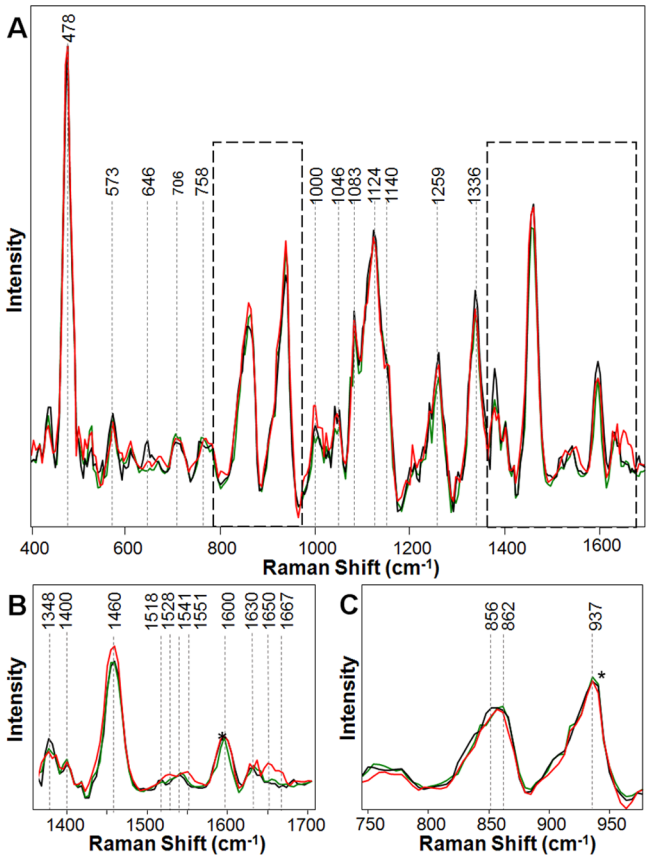

Figure 1. Raman spectra of healthy wheat grains (green), wheat grains infected by ergot (red), and black tip (black). Because of a lack of an internal standard, which can be used for spectral normalization, the reported spectra normalized on 478 cm^{-1} peak height for better visualization. Spectra in panels B and C are normalized on the 1600 $cm^{-1}$and 937 cm^{-1}, respectfully (indicated by asterisks).

observed spectral changes, we propose that pathogens associated with black tip may cause fermentation of starch to monomeric sugars. A decrease in the intensity of 1600 cm^{-1} band, originating from lignin, in the spectrum of black tip-infected wheat in suggests that pathogens that are associated with this disease induce degradation of lignin in sorghum seeds.

Raman spectra of healthy wheat and ergot exhibit a peak centered at 862 cm^{-1}. However, this peak is shifted to 856 cm^{-1} in the Raman spectrum of black tip-infected wheat (Figure 1C). This vibrational band can be assigned to the C−O−C skeletal mode of alpha glycosylic bonds in pectin compounds, which are a class of carbohydrates.[40] Pectin is synthesized methylesterified and is demethylesterified by endogenous enzymes during development.[50] In many plants, including potatoes,[51] beans,[52] and tomatoes,[53] increased methylesterified pectin is correlated with an increased ability to resist infections.[50] Therefore, the position of this vibrational band can be used to evaluate the degree of pectin methylesterification in grain. The observed shift in a frequency of this peak to 856 cm^{-1} suggests an increase in methyl esterification of pectin in the black tip infected wheat grain relative to healthy, and ergot infected wheat.[40]

Vibrational bands around 1530 cm^{-1} can be assigned to −C═C− in-plane vibrations of carotenoids (Figure 1B).[41] The longer are polyene chains of these molecules the more

Table 1. Vibrational Bands and Their Assignments for Healthy and Diseased Wheat and Sorghum Grain

band	vibrational mode	assignment
478	C−C−O and C−C−C deformations; related to glycosidic ring skeletal deformations	carbohydrates[38,43]
	δ(C−C−C) + τ(C−O) scissoring of C−C−C and out-of-plane bending of C−O	
573	δ(C−C−O) + τ(C−O)	carbohydrates[38,43]
646	ring deformations	lignin[39]
706	δ(C−C−O) related to glycosidic ring skeletal deformations	carbohydrates[38,43]
758	δ(C−C−O)	carbohydrates[38,43]
856−862	(C−O−C) skeletal mode of α-anomers	carbohydrates[40]
937−940	skeletal modes; δ(C−O−C) + δ(C−O−H) + v(C−O) α-1,4 glycosidic linkages	carbohydrates[38,43]
996−1000	ν_3(CH_3 stretching) and phenylalanine	carotenoids[41] and proteins[42]
1046	ν(C−O) + ν(C−C) + δ(C−O−H)	carbohydrates[38,43]
1083	ν(C−O) + ν(C−C) + δ(C−O−H)	carbohydrates[38,43]
1115	ν_{sym}(C−O−C), C−O−H bending	cellulose[43,44]
1124	ν(C−O) + ν(C−C) + δ(C−O−H)	carbohydrates[45]
1140−1150	ν(C−O−C), ν(C−C) in glycosidic linkage, asymmetric ring breathing	carbohydrates,[38,43] cellulose[46]
1242	C−N stretching + N−H bending, amide III	proteins[42]
1259	δ(C−C−H) + δ(O−C−H) + δ(C−O−H)	carbohydrates[38,43]
1336	ν(C−O); δ(C−O−H)	carbohydrates[38,43]
1348	δ(C−O−H)	carbohydrates[38,43]
1377	δ(C−O−H)	carbohydrates[38,43]
1400	δ(C−C−H)	carbohydrates[38,43]
1460	δ(CH) + δ(CH_2) + δ(C−O−H) CH, CH_2, and COH deformations.	carbohydrates[38,43]
1518−1551	−C═C− (in plane)	carotenoids[41,42]
1600	ν(C−C) aromatic ring + σ(CH)	lignin[47,48]
1630	C═C−C (ring)	lignin[47−49]
1650	C═O stretching, amide I α-helix	proteins[42]
1667	C═O stretching, amide I β-sheet	proteins[42]

blue-shifted this band appears in their Raman spectra. Shorter chains of polyenes, in contrast, exhibit red-shifted −C═C− vibrations. In the spectra of healthy wheat, we observe a single vibrational band of carotenoids centered at 1541 cm^{-1}. In the spectrum of ergot-infected wheat, this band is red-shifted to 1551 cm^{-1}. This suggests that growth and proliferation of this pathogen on wheat is associated with degradation and fragmentation of host carotenoids. Similar changes in carotenoid profile were observed by Baranski et al. for red tomatoes as a response to injury-induced stress.[54] We also observed a vibrational band at 1528 cm^{-1}, which was not evident in the healthy grain, indicating the appearance of a new type of polyenes in the ergot-infected wheat. Similar spectral changes have been observed for black tip-infected wheat. We observed a new carotenoid band at 1518 cm^{-1}, which is characteristic for this disease, whereas no change in frequency of 1541 cm^{-1} band was detected. These results indicate that vibrational fingerprint of carotenoids can be used to detect and identify ergot and black tip diseases on wheat.

We used multivariate data analysis to determine whether RS can be used for an accurate detection and identification of plant pathogens. Using PLS-DA, we developed a model that contained 5 components; 302 out of 512 original wave-

DOI: 10.1021/acs.analchem.8b01863
Anal. Chem. XXXX, XXX, XXX−XXX

numbers were used to generate the misclassification table (Table 2).

Table 2. Accuracy of Classification by PLS-DA for Healthy or Each Class of Diseased Wheat

	members	correct (%)	black tip	ergot	healthy	no class ($Y_{Pred} \leq 0$)
Black tip	11	100	11	0	0	0
ergot	7	100	0	7	0	0
healthy	6	100	0	0	6	0
no class	0		0	0	0	0
total	25	100	11	7	6	0
Fisher's prob.	2.3×10^{-10}					

The first three predictive components (PC) explain 8%, 30%, and 27% of the variation between classes respectively, which collectively accounts for 65% of the total class-to-class variation. The model explained 83% of the variation (R2X) in the spectra and 94% (R2Y) of the variation between the classes. Furthermore, the model correctly assigned all 24 spectra to their classes. This indicates that coupling of PLS-DA with RS allows for a high accuracy detection and identification of these two wheat pathogens.

Detection and Identification of Ergot and Mold Infection on Sorghum. In the Raman spectra of healthy sorghum grain we observed vibrational bands originating from lignin, carbohydrates, proteins, and carotenoids (Figure 2 and Table 1). Lignin shows two vibrational peaks centered at 1600 and 1630 cm^{-1}. The 1600 cm^{-1} peak can be assigned to C−C ring stretching and symmetric C−H vibration.[47] The 1630 cm^{-1} band originates from C═C aromatic ring vibration.[49] We found that these bands nearly disappear in the spectrum of mold-infected sorghum. This indicates significant degradation of lignin, associated with mold development in sorghum grain. We have also observed a decrease in the intensity of lignin peaks in the Raman spectra of ergot-infected sorghum. These findings suggest that these parasites are associated with structural modifications of grain lignin during growth and proliferation in the plant.

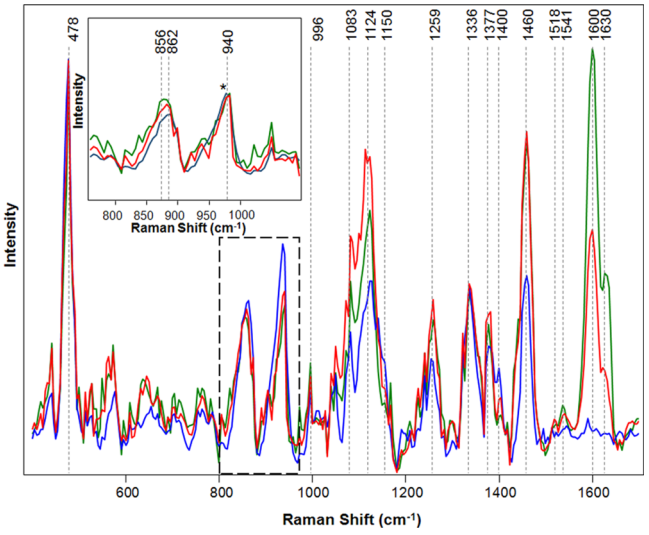

Figure 2. Raman spectra of healthy sorghum grains (green) and grains infected with mold (blue) or ergot (red). The reported spectra are normalized on 478 cm^{-1} peak height for better visualization. Insert spectra are normalized on the 940 cm^{-1} peak, indicated with an asterisk.

Carbohydrates, including monomeric sugars and starch, are the source of many vibrational bands in the spectra.[45] Vibrational bands at 1150 and 940 cm^{-1} can be assigned to C−O−C vibration, which is typical for starch. Raman bands at 1124 and 1083 cm^{-1} originate from C−O−H vibrations (Figure 2). Hydrolysis of starch produces monomeric sugars, which will be represented in Raman spectra as the increase in intensities of C−O−H vibrations. We find such an increase in C−O−C and C−O−H vibrations in the spectra of ergot (Figure 2). This indicates that pathogenic activity of these fungi in sorghum seeds is associated with fermentation of starch to monomeric sugars. At the same time, we observed that mold-related fungi caused almost the opposite changes to the equilibrium between monomeric sugars and starch. This observation suggests that mold-related pathogens are associated with the conversion of sorghum monomeric sugars into their polymeric hydrocarbons.

Another component of the Raman spectra of sorghum grain is pectin, which exhibits a vibrational band at 856 cm^{-1}.[40] We observed a red shift of this band to 862 cm^{-1} in spectra of both mold and the ergot infected sorghum (Figure 2). This suggests a decrease in methylesterification of pectin in this disease infected grain.[45,55] Methylesterification of pectin correlates an ability of plants to resist infection.[49−52] Consequently, a decrease in the methylesterificated pectin in both the mold and the ergot infected sorghum suggests a decreased ability of this grain to resist infection.

We have also observed that the ratios between the 1518 and 1541 cm^{-1} peaks change from healthy to infected sorghum grain. In the Raman spectrum of healthy grain, the 1541 cm^{-1} peak has a greater intensity. However, in both mold- and ergot-infected grains, the 1518 cm^{-1} peak increased in intensity while the 1541 cm^{-1} peak decreased. This indicates a decrease in the length of conjugated double bonds of carotenoids.[54]

Using PLS-DA, we developed a model for an accurate prediction of mold and ergot disease on sorghum. The model contained 2 predictive components; 335 out of 512 original wavenumbers were used to generate the misclassification table (Table 3).

The two PC explain 48% and 19% of the variation between classes respectively, which collectively accounts for 67% of the total class-to-class variation. The model identified lignin and carbohydrates as the strongest predictors of the sorghum pathogens, which supports the conclusions of our qualitative spectral analysis above. The model explained 92% of the variation (R2X) in the spectra and 67% (R2Y) of the variation between the classes. Furthermore, the model correctly assigned 54 out of 56 spectra to their classes. This indicates that coupling of PLS-DA with RS allows for an over 95% accurate detection and identification of these two wheat pathogens.

Middle-Stage Diagnostics of Grain Mold on Sorghum. To test whether the proposed Raman spectroscopy-based detection and identification of plant infections can be used for middle stage disease diagnostics, we analyzed mold-infected sorghum seeds at different stages of disease progression. Specifically, we analyzed healthy, middle stage and late stage infected sorghum grain (Figure 3). We observed consecutive changes in intensities and frequencies of lignin, carotenoids and carbohydrates vibrational bands in healthy,

DOI: 10.1021/acs.analchem.8b01863
Anal. Chem. XXXX, XXX, XXX−XXX

Table 3. Accuracy of Classification by PLS-DA for Healthy or Each Class of Diseased Sorghum

	members	correct (%)	mold	ergot	healthy	no class ($Y_{Pred} \leq 0$)
mold	41	100	41	0	0	0
ergot	7	71.43	1	5	1	0
healthy	8	100	0	0	8	0
no class	0		0	0	0	0
total	56	96.43	42	5	9	0
Fisher's prob.	3.6×10^{-15}					

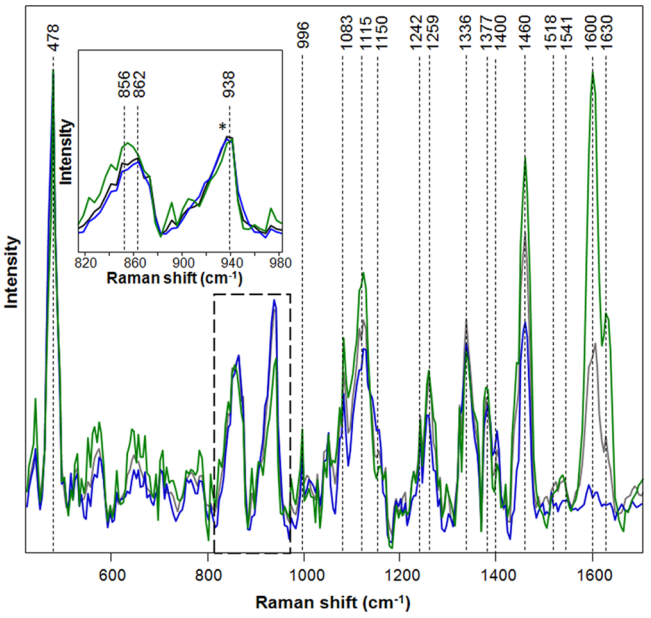

Figure 3. Different stages of progression of mold infection of sorghum grains. Raman spectra of healthy sorghum grain (green), middle progression (gray), and late stage (blue) of mold infection. Infected sorghum panicles were visually inspected and assigned to a stage of mold progression based on their appearance. The reported spectra are normalized by 478 cm^{-1} peak height for better visualization. Insert spectra are normalized on the 938 cm^{-1} peak, indicated with an asterisk.

middle, and late stage progression of mold on sorghum seeds. Specifically, we observed a gradual decrease in the intensity of lignin bands at 1600 and 1630 cm^{-1} in the spectra of middle and late stage progression of mold, indicating degradation of sorghum lignin. Similar changes were observed in vibrational bands of carbohydrates. We observed a decrease in the intensity of vibrational bands at 1460 cm^{-1}, whereas the intensities of vibrational bands at 1400 and 938 cm^{-1} increased. A shift from 856 to 862 cm^{-1} was observed for the progression of mold infection. These spectral changes point out on transformations in structure and composition of starch in the sorghum seeds that are associated with the progression of mold infection. Finally, we observed a decrease in the intensity of 1541 cm^{-1} band and an increase in intensity of 1518 cm^{-1} that are associated with carotenoids in the spectra of healthy, middle, and late stage progression of mold on sorghum grain.

We also were able to probe earlier stages of mold progression on sorghum seeds (Figure S1). These stages were categorized 1−3 (the spectrum of stage 3 is shown in Figure 3, as middle progression stage). In the spectra collected for stages 2 and 3, we observed the same trend of changes in bands' intensities, as were described above for middle and late stage mold progression (Figure 3). However, intensities of lignin and carbohydrates for stage 1 progression are significantly lower compared to stage 2 and 3. This peak observation does not follow the mold stage trend and it is presently unclear why. Further studies are currently being conducted to determine the relationship of the mold progression in stage 1 for lignin and carbohydrate peaks.

CONCLUSIONS

We have demonstrated that RS can be used for label-free, noninvasive, and nondestructive detection and identification of plant pathogens directly on intact wheat and sorghum grain. This approach allows for accurate diagnostics of simple diseases, such as ergot, which are induced by one pathogen. Moreover, using portable Raman spectrometer, we can correctly diagnose complex plant diseases such as mold and black tip. We also showed that different stages of mold infection could be distinguished. By coupling multivariate component analysis and RS, we demonstrate high accuracy in the disease detection and identification.

The portable nature of our analysis allows for utilization of RS-based detection and identification of plant pathogens on autonomous platforms, such as a robot or UAV. Constant monitoring of crops would allow for rapid detection of (and response to) disease outbreak, potentially saving billions of dollars by limiting crop damage.

ASSOCIATED CONTENT

Supporting Information

The Supporting Information is available free of charge on the ACS Publications website at DOI: 10.1021/acs.analchem.8b01863.

Different stages of progression of mold infection of sorghum grains (PDF)

AUTHOR INFORMATION

Corresponding Author

*E-mail: dkurouski@tamu.edu.

ORCID

Dmitry Kurouski: 0000-0002-6040-4213

Notes

The authors declare no competing financial interest.

ACKNOWLEDGMENTS

We are grateful to AgriLife Research of Texas A&M for the provided financial support. We also acknowledge Governor's University Research Initiative (GURI) grant program of Texas A&M University, GURI Grant Agreement No. 12-2016. We are grateful to Dr. Thomas Isakeit from the Department of Plant Pathology and Microbiology, Texas A&M University and Dr. Amir Ibrahim from the Department of Soil and Crop Sciences, Texas A&M University for the provided wheat and

DOI: 10.1021/acs.analchem.8b01863
Anal. Chem. XXXX, XXX, XXX−XXX

sorghum samples. We are also grateful to Charles Farber for the helpful discussion and assistance with graphical design.

REFERENCES

(1) Savary, S.; Ficke, A.; Aubertot, J. N.; Hollier, C. *Food Secur.* **2012**, *4*, 519−537.
(2) Sankaran, S.; Mishra, A.; Ehsani, R.; Davis, C. *Comput. Electron. Agric.* **2010**, *72*, 1−13.
(3) Raza, S. E. A.; Prince, G.; Clarkson, J. P.; Rajpoot, N. M. *PLoS One* **2015**, *10*, e0123262.
(4) Moshou, D.; Bravo, C.; West, J.; Wahlen, S.; McCartney, A.; Ramon, H. *Comput. Electron. Agric.* **2004**, *44*, 173−188.
(5) Moalemiyan, M.; Department, P. S.; Vikram, A.; Department, P. S.; Kushalappa, A. C.; Department, P. S.; Yaylayan, V. *Plant Pathol.* **2006**, *55*, 792−802.
(6) Alvarez, A. M.; Lou, K. *Plant Dis.* **1985**, *69*, 1082−1086.
(7) Chitarra, L. G.; van den Bulk, R. W. *Eur. J. Plant Pathol.* **2003**, *109*, 407−417.
(8) Wullings, B. A.; Beuningen, A. R. V.; Janse, J. D.; Akkermans, A. D. L. *Appl. Environ. Microbiol.* **1998**, *64*, 4546−4554.
(9) Lievens, B.; Brouwer, M.; Vanachter, A. C. R. C.; Cammue, B. P. A.; Thomma, B. P. H. J. *Plant Sci.* **2006**, *171*, 155−165.
(10) Li, W.; Hartung, J. S.; Levy, L. *J. Microbiol. Methods* **2006**, *66*, 104−115.
(11) Wallner, G.; Amann, R.; Beisker, W. *Cytometry* **1993**, *14*, 136−143.
(12) Padliya, N. D.; Garrett, W. M.; Campbell, K. B.; Tabb, D. L.; Cooper, B. *Proteomics* **2007**, *7*, 3932−3942.
(13) Virkler, K.; Lednev, I. K. *Forensic Sci. Int.* **2008**, *181*, e1−e5.
(14) Virkler, K.; Lednev, I. K. *Analyst* **2010**, *135*, 512−517.
(15) Virkler, K.; Lednev, I. K. *Anal. Chem.* **2009**, *81*, 7773−7777.
(16) Liu, B. H.; Han, G. M.; Zhang, Z. P.; Liu, R. Y.; Jiang, C. L.; Wang, S. H.; Han, M. Y. *Anal. Chem.* **2012**, *84*, 255−261.
(17) Schmidt, H.; Sowoidnich, K.; Kronfeldt, H.-D. *Appl. Spectrosc.* **2010**, *64*, 888−894.
(18) Zeng, Z. C.; Hu, S.; Huang, S. C.; Zhang, Y. J.; Zhao, W. X.; Li, J. F.; Jiang, C.; Ren, B. *Anal. Chem.* **2016**, *88*, 9381−9385.
(19) Zhou, X. J.; Jiang, D.; Xu, J.; Xu, Y.; Wang, S. X. Handheld Raman spectrometer. U.S. Patent USD748510S1, 2016.
(20) Rigaku Corporation. Advanced handheld Raman Spectrometer, 2018. https://www.rigaku.com/en/progeny.
(21) Kurouski, D.; Van Duyne, R. P. *Anal. Chem.* **2015**, *87*, 2901−2906.
(22) Hager, E.; Farber, C.; Kurouski, D. *Forensic Chem.* **2018**, *9*, 44−49.
(23) Jehlička, J.; Culka, A.; Baštová, M.; Bašta, P.; Kuntoš, J. *Philos. Trans. R. Soc., A* **2016**, *374*, 20160042.
(24) Košek, F.; Culka, A.; Jehlička, J. *J. Raman Spectrosc.* **2017**, *48*, 1494−1502.
(25) Farber, C.; Kurouski, D. *Anal. Chem.* **2018**, *90*, 3009−3012.
(26) Audilakshmi, S.; Stenhouse, J.; Reddy, T. *Euphytica* **2000**, *116*, 95−103.
(27) Dixon, J.; Braun, H. J.; Kosina, P.; Crouch, J. H. In *Wheat Facts and Futures 2009*; International Maize and Wheat Improvement Center: Mexico, 2009; Chapter 1-25, p 95.
(28) Oerke, E. *J. Agric. Sci.* **2006**, *1*, 31−43.
(29) Gworgwor, N. A.; Weber, H. C. *Mycorrhiza* **2003**, *13*, 277−281.
(30) Scheffer, J.; Tudzynski, P. *Mycol. Res.* **2006**, *110*, 465−470.
(31) Miedaner, T.; Geiger, H. H. *Toxins* **2015**, *7*, 659−678.
(32) Rule number 810.256 Grades and Grade Requirements for Oats. *The Code of Federal Regulations of the United States of America*; Office of the Federal Register, U.S. Government Printing Office, 1982.
(33) Watkins, J. *Black Point Disease of Wheat*; University of Nebraska-Lincoln Extension, Institute of Agriculture and Natural Resources, 2005; http://www.totoagriculture.org/PDFs/PlantDiseasesPests/41.pdf.
(34) French, R. *Potential Wheat Disease Issues on Seed, Seedlings, and Heads during a Wet Year (2015)*; Texas A&M AgriLife Extension, 2015; http://agrilife.org/amarillo/files/2015/12/Potential-Wheat-Disease-Issues-on-Seed-Seedlings-and-Heads-During-a-Wet-Year.pdf.
(35) Thakur, R. P.; Reddy, B. V. S.; Indira, S.; Rao, V. P.; Navi, S. S. Sorghum Grain Mold. Plant Pathology and Microbiology Publications, 2006. https://lib.dr.iastate.edu/cgi/viewcontent.cgi?referer=https://www.google.com/&httpsredir=1&article=1001&context=plantpath_pubs.
(36) Audilakshmi, S.; Das, I. K.; Ghorade, R. B.; Mane, P. N.; Kamatar, M. Y.; Narayana, Y. D.; Seetharama, N. *Crop Prot.* **2011**, *30*, 753−758.
(37) Kurouski, D.; Van Duyne, R. P.; Lednev, I. K. *Analyst* **2015**, *140*, 4967−4980.
(38) De Gussem, K.; Vandenabeele, P.; Verbeken, A.; Moens, L. *Spectrochim. Acta, Part A* **2005**, *61*, 2896−2908.
(39) Jentzsch, P.; Ramos, L.; Ciobotă, V. *Cosmetics* **2015**, *2*, 162−176.
(40) Szymańska-Chargot, M.; Chylińska, M.; Pieczywek, P. M.; Rösch, P.; Schmitt, M.; Popp, J.; Zdunek, A. *Planta* **2016**, *243*, 935−945.
(41) Adar, F. *Spectroscopy* **2017**, *32*, 12−20.
(42) Devitt, G.; Howard, K.; Mudher, A.; Mahajan, S. *ACS Chem. Neurosci.* **2018**, *9*, 404−420.
(43) Edwards, H. G. M.; Farwell, D. W.; Webster, D. *Spectrochim. Acta, Part A* **1997**, *53*, 2383−2392.
(44) Agarwal, U. P.; Ralph, S. A. *Appl. Spectrosc.* **1997**, *51*, 1648−1655.
(45) Almeida, M. R.; Alves, R. S.; Nascimbem, L.; Stephani, R.; Poppi, R. J.; de Oliveira, L. F. C. *Anal. Bioanal. Chem.* **2010**, *397*, 2693−2701.
(46) Garside, P.; Wyeth, P. *Stud. Conserv.* **2003**, *48*, 269−275.
(47) Kang, L.; Wang, K.; Li, X.; Zou, B. *J. Phys. Chem. C* **2016**, *120*, 14758−14766.
(48) Agarwal, U. P. *Planta* **2006**, *224*, 1141−1153.
(49) Pompeu, D. R.; Larondelle, Y.; Rogez, H.; Abbas, O.; Pierna, J. A. F.; Baeten, V. *Biotechnol. Agron. Soc. Environ.* **2017**, *22*, 1−16.
(50) Lionetti, V.; Cervone, F.; Bellincampi, D. *J. Plant Physiol.* **2012**, *169*, 1623−1630.
(51) McMillan, G. P.; Hedley, D.; Fyffe, L.; Perombelon, M. C. M. *Physiol. Mol. Plant Pathol.* **1993**, *42*, 279−289.
(52) Boudart, G.; Lafitte, C.; Barthe, J. P.; Frasez, D.; Esquerre-Tugaye, M.-T. *Planta* **1998**, *206*, 86−94.
(53) Wydra, K.; Beri, H. *Physiol. Mol. Plant Pathol.* **2006**, *68*, 41−50.
(54) Baranski, R.; Baranska, M.; Schulz, H. *Planta* **2005**, *222*, 448−457.
(55) Sene, C. F. B.; McCann, M. C.; Wilson, R. H.; Grinter, R. *Plant Physiol.* **1994**, *106*, 1623−1631.

DOI: 10.1021/acs.analchem.8b01863
Anal. Chem. XXXX, XXX, XXX−XXX